

# Thermal Design of a Fusion Power Plant and Its Waste Heat Recovery to Produce Hydrogen

**Bozorgian, Alireza\*<sup>+</sup>**

*Department of Chemical Engineering, Mahshahr Branch, Islamic Azad University, Mahshahr I.R. IRAN*

**Norouzi, Nima**

*Department of Energy Engineering and Physics, Amirkabir University of Technology (Tehran Polytechnic), Tehran, I.R. IRAN*

**ABSTRACT:** As climate change becomes a more severe problem each day, the need to respond to it firmly grows in importance. For decades many scientists believed fusion, or, as it is called in the engineering society, the artificial sun was the future of unlimited clean and cheap energy sources. Since 2007 when the international nuclear fusion research and engineering megaproject started as a mega cooperation project between several industrial countries, this ambition seemed to be at hand more than at any other time. This mega project was a turning point for the fusion sub-projects to emerge in many countries and regions. But as fusion projects grow in number, similar to all other energy systems, a need to analyze the using second law of thermodynamics comes a great matter of importance. This paper aims to study the European demonstration fusion power reactor pulse integrated power plant and its waste heat recovery potential to produce hydrogen, considering the primary heat transfer system, the intermediate Heat Transfer System, including the Energy Storage System's first option to ensure power continuity. This study shows that the fusion power plant is among the most efficient stand-alone energy systems with an overall efficiency of (85.07 and 89.1% in energy storage and auxiliary heater arrangements, respectively). Using waste heat assessments to produce hydrogen resulted in even more efficient plants and an increase of the plant's overall efficiency to more than 94.15 and 92.05% in energy storage and auxiliary heater arrangements, respectively, close to the Carnot efficiency of a similar ideal plant, and means that the irreversibility is in its minimum state.

**KEYWORDS:** Methane reforming; Sustainable energy; EU-DEMO; Molten salt stabilizer; Energy storage system; Fusion Hydrogen,

## Introduction

For some decades, it has been considered that the process that energizes the sun - nuclear fusion - would solve the earth's energy problems. It remains to be seen

whether nuclear fusion meets our expectations, as fusion power plant designers face complex technological problems, and no such plant has yet been built. However,

---

\* To whom correspondence should be addressed.

+ E-mail: alireza.bozorgian@iau.ac.ir

1021-9986/2023/2/538-557

20/\$/7.00

remarkable progress has been made in taking advantage of the possibilities offered by mergers. For decades, research in the areas of nuclear fusion has been carried out in various countries. Efforts have yielded significant results in improving plasma confinement; the Tokamak experiment has reached unsurpassed plasma pressure values relative to the magnetic field pressure Tokamak Fusion Test Reactor (TFTR), which has generated 10 million watts of thermal energy from fusion. The Joint European Torus (JET) is expected to achieve similar conditions, where the generated fusion energy exceeds the input energy. The International Thermonuclear Experimental Reactor (ITER), designed by experts from the European Community, Japan, the Russian Federation, and the United States, will have to solve outstanding physics problems, such as plasma purity and interruptions, and to sustain current. Over time, there is confidence that technical design problem - including those related to magnets - can be solved in superconductors, vacuum systems, cryogenic systems, plasma heating systems, plasma diagnostic systems, and fertile layer cooling systems. Other important aspects of fusion power plant design have to do with safety and economics. This article examines the safety issues in the design of fusion power plants and their efforts in safety-related areas through international cooperation activities.

Demonstration fusion power reactor is a study concentrated on developing a prototype fusion plant to generate electricity. This is a link between the ITER and commercial electricity markets. The project's roadmap considered several options and selections for achieving those aims and targets. Most of the literature in this field considers four options to achieve sun-to-power energy conversion. One of them is the primary heat transfer system or Primary Heat Transfer System studied by *Federici et al.* [1, 2]. *Cismondi et al.* [3] suggest using a helium-cooled pebble bed breeding blanket. According to the technical concept, the reactor system's Demonstration fusion power reactor needs to operate in two modes of pulse and dwell. The plasma state is induced in the pulse mode because of an increasing current in the solenoid and dwells mode when the existing current reaches its maximum amount. Briefly, in a technical view, a pulse occurs when the fusion reaction occurs, and dwell is when the heat decays between two fusion pulses. *Bachmann et al.* [4] studied breeding blankets, which are the most important parts

of the system where the lithium is converted to generate tritium. *Federici* [2] also mentioned a proposed diverter and vacuum vessel arrangement, which is considered the secondary heat source (notable that the temperature and heat flux reached to those secondary sources is much lower than the primary one). *Linares* [5] and *Barucca* [6] also proposed an energy storage system in the intermediate heat-transfer cycle to ensure constant power generation during pulses and dwells. *Bubelis et al.* [7] studied the Rankine system as a possible power generation option considered the most reliable. *Linares* [5] proposed using supercritical CO<sub>2</sub> Brayton cycles as a suitable cooling system for the breeding blanket system and power generation. *Malinowski et al.* [8] used the Rankine system as a power cycle and placed a water-cooled system for the breeding blanket.

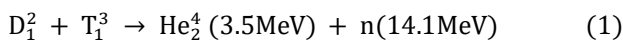
The literature in this field was considered in the previous paragraphs, and the main points of their contribution are also presented. The first research gap considered in this field is that the power cycle, the most important aim of the whole concept, is not considered a primary literature aspect. The second gap detected is that the thermodynamic aspects of the overall fusion power systems like the EU- Demo fusion power reactor were never studied to detect the power loss sources in the light of the first and second laws of thermodynamics concept. The third gap is the exergy analysis implementation on the system, which is very important because of the high-temperature processes during the system's operation (causing enormous exergy destruction). Thus, as mentioned in the concept of exergy analysis, where there is a significant temperature variation, a significant irreversibility and exergy destruction occurs that can be recovered and used in other beneficial processes.

This paper aims to consider and fill those gaps in the fusion power systems' research body. First of all power generation is the primary focus of this paper, and all aspects of it were considered in detail. Second, the exergy analysis and the concept of the second law of thermodynamics are used in this paper to investigate the overall performance of the European Demonstration fusion power reactor system for power generation. The main exergy destruction sources are detected using the entropy concept. Using the exergy analysis results helps find the main heat loss sources and proposes an additional arrangement to use that leakage more beneficially.

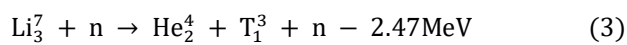
A methane reforming system is proposed and designed in this paper to achieve that goal and enhance the system's overall performance.

### **European Prototype Demonstration fusion power reactor**

European Demonstration fusion power reactor [1] is a pulsed fusion power plant under design in the Euro fusion consortium's cooperation framework (ITER Project). Because the atomic hydrogen fusion reaction needs an enormous available volume to become implementable, the nuclear fusion with the most suitable characteristics for industrial use is the reaction between deuterium and tritium [2]:



The production of tritium, which is not available in the needed value to fuel the reaction, is produced employing a breeding nuclear reaction that is made available with Lithium nuclei, stored in the blanket of the plasma chamber, according to the following reactions [2]:



These reactions, ensuring the nuclei fusion system's continuity, rely on the Tritium generation inside the blanket's Breeding blanket, where thermal electricity is produced further to the quantity generated utilizing neutrons within the First Wall. The breeding blanket and First Wall are components of the primary heat transfer systems and contribute to the overall thermal power conveyed to the power Conversion system, generating the electric strength launched to the outside grid. Predominant standards are surely proposed and developed for the European Demonstration fusion power reactor: Helium-Cooled Pebblebed and Water-Cooled Lithium Lead [3]. The Water-Cooled Lithium Lead concept was selected as a reference in this paper is primarily based on liquid lithium-lead eutectic as breeder and water to eliminate the generated heat (through tubes inserted into the Breeding blanket and into the First Wall). The Breeding blanket and First Wall number one heat switch structures are water circuits derived from the Pressurized Water Reactors (PWR) fission power plant generation, capable of providing steam for the turbine.

Other additional heat assets are the diverter and the vacuum vessel. However, the electricity generated is restrained and at low temperatures (131– 211°C). Thus, it isn't always feasible to use Diverter and the vacuum vessel energy to supply steam and then are used as feedwater regeneration preheaters to elevate the electric efficiency. The European Demonstration fusion power reactor Water-Cooled Lithium Lead 2017 configuration [4] has been used within the calculations.

The demonstration fusion power reactor is designed to operate in a pulsed mode via alternated stages similar to a plasma burn and a dwell duration. This running collection implies that the production of thermal strength in a Breeding blanket and First Wall of the reactor, and launched to the Primary Heat Transfer System, is not non-stop, and therefore, this doesn't guarantee continuity within the shipping of electricity from the Power Conversion System to the power grid. The period of plasma burn mode (pulse section) is two hours, while the duration of decreased heating energy mode (dwell duration) is 10 mins throughout, which best produces the decay warmth. The decay heat is approximately identical to at least one% of the response heat produced for the duration of pulse mode, for that reason developing a discontinuity in electrically powered power launch.

An Intermediate heat transfer system is foreseen to offer non-stop power generation. This answer in the layout of the Demonstration fusion power reactor and the related stability of the plant has caused a configuration of the Intermediate heat transfer system constituted with the aid of the secondary aspects of Intermediate warmth Exchangers and the heat storage system, which includes two molten salt tanks operating at exceptional temperatures [4]. Here, compared with the molten salt energy storage system, an opportunity alternative is represented through a natural fuel (methane) fired boiler designed to generate the superheated steam conveyed to excessive- and coffee-stress steam turbines. Fig. 1 indicates a simplified system flow diagram of the entire device and major systems and additives constituting the plant with energy storage system configuration below evaluation.

### **Energy storage system arrangement**

The energy storage system is part of the Intermediate heat transfer system designed to feed the Power Conversion System, freeing steady-state power to the grid.

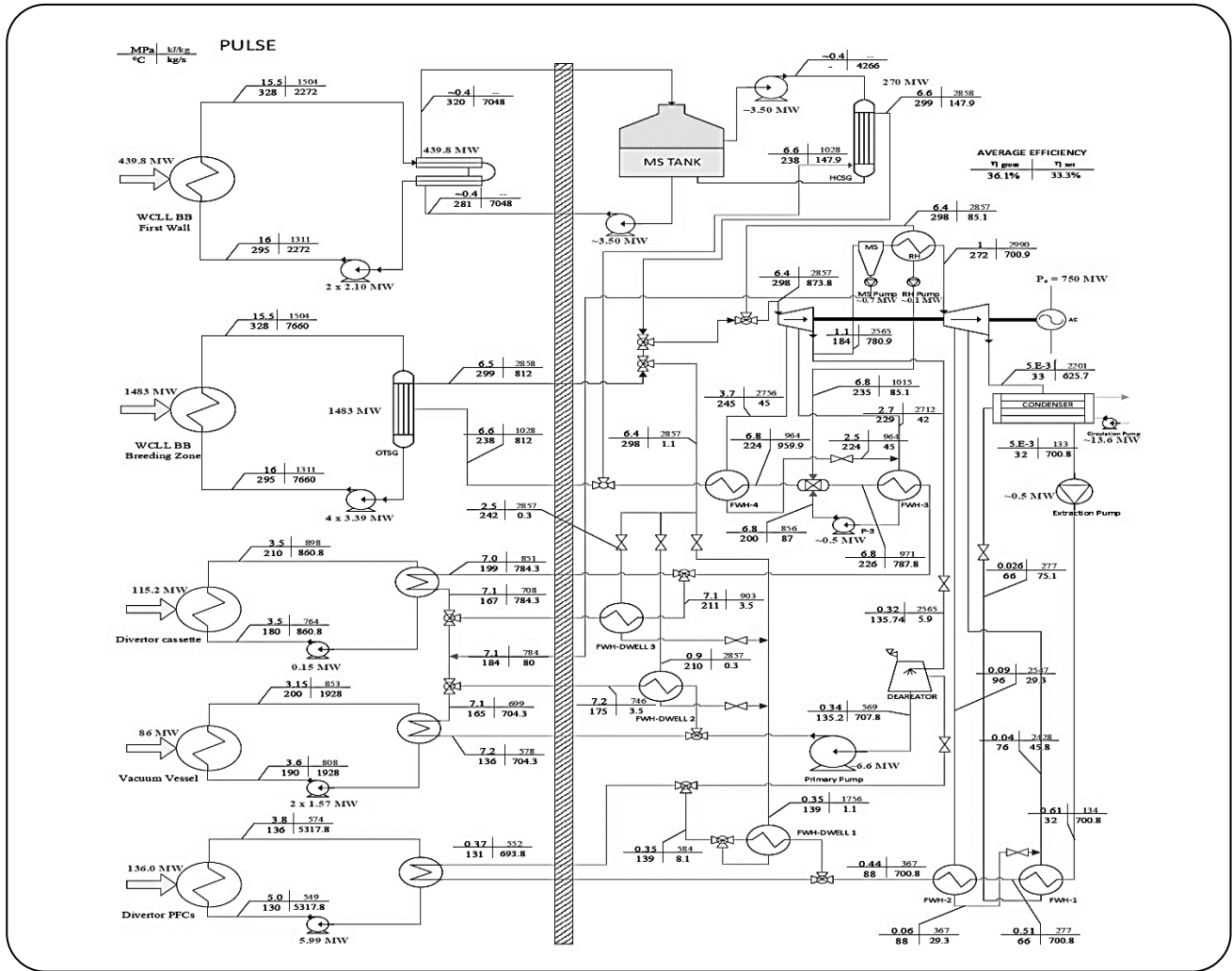


Fig. 1: Schematics of European Demonstration fusion power reactor plant (source: ITER Project).

The present-day layout of the energy storage system is constituted through exclusive tanks crammed in with molten salt and related employing a pipeline wherein molten salt flows in two directions relying upon the working section of the reactor [4]. in the course of the pulse phase, the molten salt is moved from the Lesser temperature tank to higher temperature tank after heat transfer with the cooling water conveyed from the First Wall Primary Heat Transfer System. The hot tank saves the high-temperature molten salt heated thru two intermediate water-salt heat exchangers. The Lesser temperature tank recovers the low-temperature molten salt cooled during the reside phase to provide the superheated steam conveyed to the power plant's turbines. This configuration calls for the pumping of molten salt from the Lesser temperature tank to a higher temperature tank

in the course of dwell mode and vice versa at some stage in the alternative model.

Because molten salt is concerned, HITEC is the commercial product of a ternary salt characterized by chemical, physical and thermodynamic properties appropriate for manner situations asked via the energy storage system plant. HITEC is a eutectic aggregate of water-soluble and inorganic salts of potassium nitrate  $KNO_3$ , sodium nitrate  $NaNO_3$  and sodium nitrite  $NaNO_2$  [5] with the subsequent composition: 7.02 % of  $NaNO_3$ , molecular weight 84.99 g/mol; 40.05 % of  $NaNO_2$  molecular weight 69.05 g/mol; 53.1 % of  $KNO_3$  molecular weight 101.103 g/mol; the molecular weight of the aggregate same to 87.1 g/mol [6].

The energy storage system design relies on the subsequent parameters characterizing the physical

properties and molten salt's behavior at some stage in the heating and cooling stages: liquid segment-specific heat, melting-solidification latent heat, most allowable temperature, solidification temperature, viscosity  $v/s$  temperature, salt mass used in energy storage system [7].

HITEC molten salt's precise warmness at steady stress is  $cp = 1.55 \text{ kJ}/(\text{kg}\cdot\text{K})$ , and it's suggested to be considered a constant price with temperature independence. However, the must-have literature expressions [6] to calculate enthalpy and entropy for energy storage system layout [8].

In the course of the pulse (2 h), the Breeding blanket Primary Heat Transfer System thermal energy (1484  $MWth$ ) is brought to the power plants. The First Wall Primary Heat Transfer System supplies thermal energy of 440  $MWth$  to the energy storage system: a fragment of this strength is transferred to the desktops, 266  $MWth$ , and 174  $MWth$  are stored during the pulse phase corresponding to a stored strength of  $1.25 \cdot 10^6 MJ$  to be added to the power plants during the reside time [9]. Throughout the pulse length, the thermal power is transferred from the energy storage system to the power plants thru one Helical Coil Steam Generator [10]. The new molten salt flows in the shell side and transfers thermal energy to water flowing inside the tube. The molten salt temperature cycle is  $280 - 320 \text{ }^\circ\text{C}$ . The feedwater enters the Helical Coil Steam Generator with an inlet temperature of  $238 \text{ }^\circ\text{C}$  and exits with an outlet temperature of  $300 \text{ }^\circ\text{C}$  at 6.4  $MPa$ . The Helical Coil Steam Generator mass going with the flow charge of HITEC is 4375.4  $kg/s$ , and the feedwater mass flow rate, calculated with the enthalpy balance, is 284  $kg/s$  [11].

At some point in the dwell time (600 s), the mass flow of molten salt from high to low-temperature tanks is 33437  $kg/s$ . The energy storage system tank includes 20063 ton of molten salt at the beginning of residing. Thus approximately 11001  $m^3$  are needed to keep this mass. In this phase, the energy storage system offers strength to power plants thru 4 Helical Coil Steam Generators [12]. The average power to be had in dwell mode is approximately 2087  $MWth$ . Accordingly, the energy of every Helical Coil Steam Generator is 521  $MWth$ . It's far noteworthy that one out of the 4 Helical Coil Steam Generators is the only one working in the course of pulse time to transmit 266  $MWth$ , as described. The thermal energy recovered from Divertor Cassette, Divertor Plasma dealing with additives (power components), and Vacuum Vessel are used in the feedwater regenerative preheating

through specifically designed heat exchangers. Discern one shows the Primary Heat Transfer System boundary conditions accounted for within the power plants' layout finished *via* the GateCycle<sup>TM</sup> application. The output statistics and facts have been amassed in a spreadsheet right here, followed by interest calculations. The objective of the existing observation is to provide the second law of thermodynamics evaluation of all additives based totally on the exergy method to adopt a rigorous and entire technique to evaluate dissipation phenomena impacting the plant's efficiency.

#### **Auxiliary natural gas steam generator**

An alternative option to the energy storage system, evaluated and compared with the energy storage system, includes an auxiliary natural gas (methane) fired steam generator to produce superheated steam throughout the dwell section [13]. The steam generator's layout parameters are derived from the fusion reactor's process statistics, considering that the thermal electricity to be released in the stay segment to make certain the continuity is a few 254  $MW$  corresponding to the ten% of the thermal electricity produced all through pulse mode [14]. It's far assumed a thermal electricity performance same to 86% thinking that the economizer lacks since the feedwater preheating happens using the heat interplay in diverters and vacuum vessels. The gas considered within this analysis is 100% methane with a Low Heating Value (LHV) equal to  $802.2 \text{ kJ}/\text{mol} = 50147 \text{ kJ}/\text{kg}$  [15]. The auxiliary boiler is thought to function at rated power at some point in each pulse and dwell mode. Certainly, the consistent obligation prevents thermal fatigue and represents an additional thermal energy contribution for pulse mode duration [16, 17].

#### **Hydrogen generation configuration**

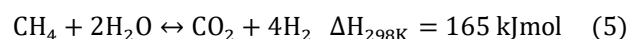
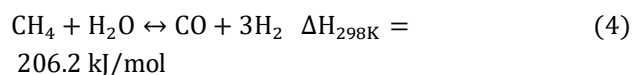
Hydrogen is one of the most important materials needed in refining crude oil, chemical processes of hydrogenation, Hydrodesulphurization, and production of methanol, ammonia, etc. Besides, hydrogen is the most important factor of pure energy for hydrogen [18]. Fuels are also required to generate electricity with 45-55% efficiency and reduce acidic gas emissions. Hydrogen is a colorless, odorless substance with the lightest chemical element and has the most optimal fuel-to-weight ratio in all fuel types. It is also used in chemical processes such as

dehydrogenation of fats and oil dihydroalkylation. In recent decades, the tendency to hydrogen has been a turning point for controlling the earth's temperature [19]. The growth of global energy demand over the 21st century has always led to a new energy carrier's arrival to reduce greenhouse gas emissions. And all those necessities have led to the hydrogen industry emergence. Nowadays, 18% of hydrogen is produced using petroleum, 30% uses coal, 48% uses natural gas, and only 4% is produced using electricity [20].

The use of hydrogen as a fuel or secondary carrier in fuel cells has the highest efficiency of gas-to-electricity conversion on a small scale. In fuel cells, the only product of hydrogen fuel is water. Using this technology will significantly reduce the amount of  $\text{NO}_x$  and  $\text{CO}_x$  of solid particles and other pollutants released from fossil fuels' burning [18].

The reforming reaction of heavier hydrocarbons with water vapor is the main process for hydrogen production. Although natural gas (methane) has become the most important and economical raw material today, hydrocarbons' reforming reaction with steam is still very attractive for the chemical and petrochemical industries [20]. This attraction is especially evident in places where not enough methane is found, such as Japan and the United States.

This paper investigates the process of hydrogen production by methane reforming in membrane-fluidized bed reactors. Membrane reactors are generally composed of concentric tubes, one of which is the membrane. The membrane is usually made of palladium or palladium-silver alloy, which is only permeable to hydrogen. Therefore, in membrane reactors, hydrogen is constantly separated from the reaction site, the chemical equilibrium is shifted, and the operation remains at a moderate temperature. Also, the membrane properties are an increase in the conversion percentage and a decrease in CO selectivity. Methane conversion reactions include the following [21]:



The result is the production of syngas gas (a mixture of  $\text{CO}$  and  $\text{H}_2$ ), in which the catalytic reaction of  $\text{CO}$  with  $\text{H}_2\text{O}$  is performed to produce  $\text{H}_2$  and  $\text{CO}_2$ . This necessary step includes a low-temperature shift (LTS) at 190-210°C [1] and then a high-temperature shift at 350°C (High-temperature shift, HTS). Ref. [19-25] investigated methane vapor reforming in a membrane-fluidized bed reactor. The first part of the reactor used, which is the reaction site, in which the nickel catalysts reactions (1) and (2) are largely endothermic, while reaction (3) is slightly exothermic. Considering the Loshatelier principle and the matter balance in the first two reactions, the pressure drop causes the reaction to proceed while the pressure does not affect the reaction (3) considering the Loshatelier principle and the matter balances the first two reactions. The  $\text{CO}_2$  accumulation from the reactor is another option to increase methane conversion. The reactor used is divided into two parts. The first part is the reaction site, it contains an alumina-based nickel catalyst ( $\text{Ni-Al}_2\text{O}_3$ ) with a fixed solid fraction (solid volume to the total volume of the catalyst). The feed stream consists of methane and vapor, which enter the fluidized bed as a plug. The second part is where the hydrogen broom penetrates, and nitrogen gas is used as the broom. The heat required for the reaction is given to the reactor as the heat required for the external heat reaction. This process's equations are modeled [21] and solved with Aspen Hysys software, given below (see Fig. 2) [26].

In this paper, the waste heat of the different modes of fusion plants are used to fuel the reforming process, and its effect on the exergy, energy and price of energy produced in the plant is analyzed, respectively.

## THEORETICAL SECTION

The literature reviews definitions and applications referring to properties underpinning the exergy approach and the second thermodynamics evaluation [7-8]. Thermal power transfer's contribution largely characterizes the energy storage system by utilizing heat interactions in different exchanges. Further, the mechanical exergy balance is accounted for. Calculation of exergy is based on the technical conditions and properties deriving from the Intermediate heat transfer system layout and optimization; all facts and statistics regarding move interested by the present verification analysis of the Intermediate heat transfer system are suggested within the literature [1]

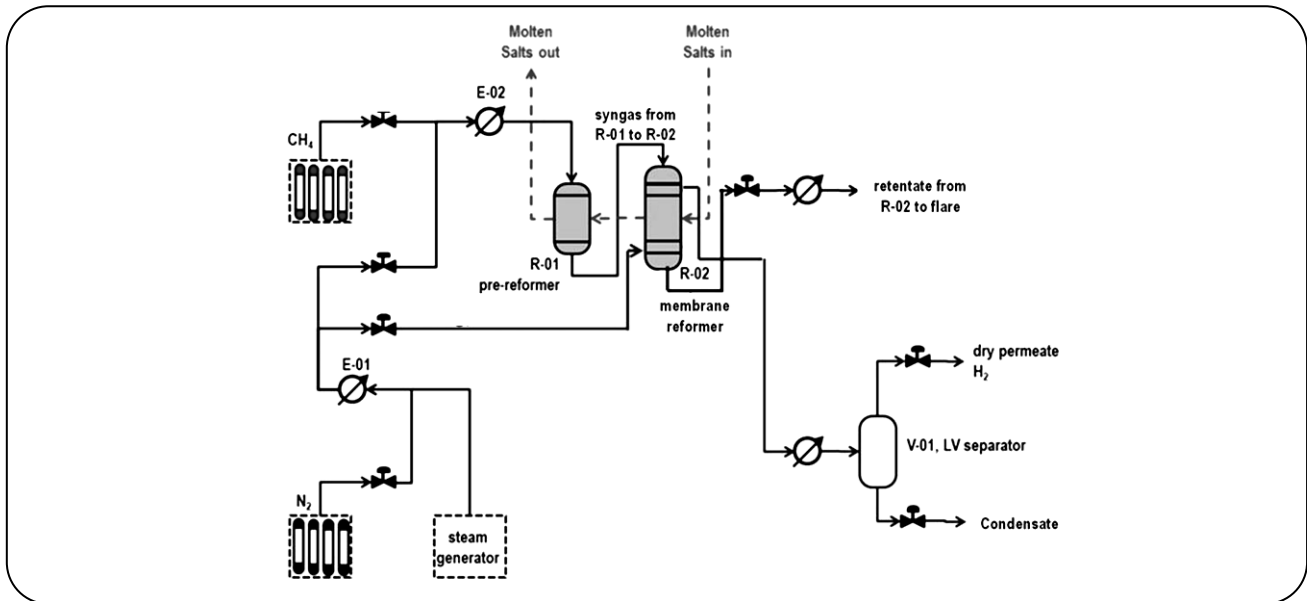


Fig. 2: Schematics of the solar membrane methane reforming for hydrogen production.

because of the result of a design mission. As a result, plant components' dimensions and materials are not directly involved in this exergy analysis and aren't addressed alongside calculations. In the end, the exergy stability is received from the algebraic sum of contributions referring to all components constituting the energy storage system [27].

As long as the dissipation processes are concerned, the warmth and mass interplay flow internally to water, and molten salt is left out. Options are taken into consideration for the computers delivered all through dwell phase:

(1) energy storage system with molten salt high and low-temperature tanks; (2) methane fuelled fired boiler for steam generation. As some distance as the reference source  $R$  is involved, the environment conventional situations corresponding to 298 K and 1 bar are assumed. Consequently, water is in the sub-cooled liquid state, and its reference thermodynamic characteristics to calculate exergy are the specific enthalpy  $h_R = 104.88 \text{ kJ/kg}$  and the specific entropy  $s_R = 0.366 \text{ kJ/(kg K)}$ . Among those thermodynamic characteristics of molten salt within the liquid phase implied within the exergy evaluation, the following expressions are right here followed for enthalpy and entropy [28]:

$$h - h_R = \int_{298.15}^{\text{Melt}} c_p dT + \Delta h_{\text{MELT}} + \int_{T_{\text{melt}}}^T c_p dT \quad (7)$$

$$= 0.8 \times 10^{-1} T^2 + 27.75T - 14568.9 \frac{\text{J}}{\text{mol}}$$

$$s - s_R = \int_{298.15}^{T_{\text{melt}}} \frac{c_p}{T} dT + \frac{\Delta h_{\text{MELT}}}{T_{\text{melt}}} + \quad (8)$$

$$\int_{T_{\text{melt}}}^T \frac{c_p}{T} dT = 1.6 \cdot 10^{-1} T + 27.75 \ln T - 202.83 \text{ J/mol.K}$$

These characteristics are estimated concerning the reference source parameters and are specially defined to estimate the energy storage system's exergy balance [29]. The above functions' numerical result functions are divided by the molten salt's molecular weight of molten salt to obtain  $k/\text{kg}$  and  $k/\text{(kgK)}$  respectively to ensure consistency with the unit of measurement system adopted [30]. Calculations have been carried out based on the GateCycle™ program output resulting from the plant configuration design described in the process flow diagram [31]. The canonical definition of particular physical exergy for open bulk flow structures, thru the control extent defining the contributing streams to the plant, is the subsequent [31-36]:

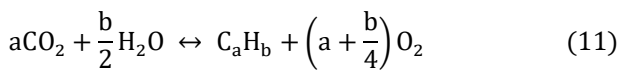
$$ex_T = (h - h_R) - T_R(s - s_R) \quad (9)$$

in which  $h$  and  $s$  are the specific enthalpies, and particular entropy at the system's generic thermodynamic circumstances, and  $h_R$  and  $s_R$  are the same characteristics at the reference source parameters of the reservoir represented by using the surroundings. The above expression evaluates the exergy balance of all Thermal

Energy exchangers operating inside the plant. As a way because of the thermal exergy rate, the following expression is adopted that accounts for mass flowrates [37]:

$$EX_T = \dot{m}(h - h_R) - T_R(s - s_R) \quad (10)$$

The evaluation of performances supplied with the aid of the two plant configuration alternatives below discussion needs to assess the chemical exergy of the auxiliary boiler's methane combustion process. The canonical definition of specific molar chemical exergy for open structures is adopted to achieve this. The unique case of hydrocarbons may be treated considering the subsequent usual combustion reaction [38]:



It is predicated on the molar fractions of parts of substances and is expressed in the form here mentioned [39] based totally on the distinction of hydrocarbon chemical potential  $\mu$  before and after the response on the reference source represented with the aid of the environmental reservoir  $R$ [40-45]:

$$ex_{CaHb}^C = \mu_{CaHb} - \mu_{CaHb}^R = \left[ g_{CaHb} + \left(a + \frac{b}{4}\right)g_{O_2} - ag_{CO_2} - \frac{b}{2}g_{H_2O} \right]_{TR,PR} + RT_R \ln \left[ \frac{(x_{O_2}^R)^{\frac{a+b}{4}}}{(x_{CO_2}^R)^a + (x_{H_2O}^R)^{\frac{b}{2}}} \right] \quad (12)$$

Wherein  $x_i$  is the molar fraction of each  $i$ -th constituent appearing within the equation and  $g_i$  is the molar Gibbs chemical capacity at general conditions of  $T_R = 298.15 K$  and  $P_R = 101.325 kPa$ .

Using mechanical exergy is mainly devised and followed to assess steam turbines' second law performance [9-10]. The mechanical exergy does not account for the working fluid mass kinetic electricity and gravitational or electro-magnetic capability power of the entire mass referred to as its point of gravity. These components termed kinetic exergy and capability exergy, are omitted when thinking about a plant's balance. Then, mechanical exergy accounts for inner mechanical energy  $u^M = u(p) = -pV$  that depends on pressure and volume coming into and exiting the manipulated volume identifying the elemental system-level working and an adiabatic manner of a steam turbine. An adiabatic

reversible process is defined as isentropic in that no heat interactions occur along the expansion (or compression) process. Then, the thermal exergy, described in terms of maximum internet beneficial work, with a null variant of entropy inside the expression  $ex^T = (h - h_R) - T(s - s_R)$ , ought to be coincident with the enthalpy change between entering and output states,  $\Delta ex^T = W = h_{OUT} - h_{IN}$ . This definition concerns thermal exergy related to the thermal inner energy  $u^T = u(T) = Ts$  while the adiabatic expansion freeing inner work is related to the mechanical element of inner power. Instead, the mechanical exergy ought to be described because the most internet useful thermal energy depends on the difference of internal mechanical power between inlet and outlet running fluid states. The definition  $ex^M = (h - h_R)^M + p_{RV_R}(s^M - s_R^M)$  is appropriate to assess this functionality related to strain and the extent with appreciation to pressure and precise extent of the reference source of the reservoir. The equation  $p_R(s^M - s_R^M)$  represents the mechanical exergy loss or the non-beneficial work launched to the reservoir at  $p_{RV_R}$ . Indeed, this part accounts for the fact that, even though the variation of enthalpy equals the work interplay launched to the outside environment, the functionality in terms of work-to-heat conversion via and the best cycle is not equal because of the distinctive pressure-to-volume correlation that determines a different available mechanical internal power. The energy loss in phrases of non-beneficial work interplay launched to the reservoir needs to be accounted for within the exergy balance of steam turbines. Therefore, for a steam turbine stage, the following equations follow:

$$ex_{IN}^M = h_{IN} + p_{RV_R}(s_{IN}^M - s_R^M) \quad (13)$$

$$W_{OUT}^{EXT} \Leftrightarrow ex_{OUT}^M = (Q_{IN \rightarrow OUT}^{AR})_{WORK}^{MAX} ex_{OUT}^M = \quad (14)$$

$$h_{OUT} + p_{RV_R}(s_{OUT}^M - s_R^M) \quad (15)$$

The steam turbine mechanical exergy stability alongside a real method is the following:

$$\Delta ex_M = \Delta ex_M^{REV} + \Delta ex_M^{IRR} = (h_{OUT} - h_{IN}) + p_{RV_R}(s_{OUT}^{REV} - s_{IN}^{REV})^M + p_{RV_R}(s^{IRR})^M \quad (16)$$

in which the function  $p_{RV_R}(s^{IRR})^M$  represents mechanical exergy destruction.

Real approaches imply irreversible phenomena determining an amount of entropy generation. The Gouy-

Stodola theorem ensures the direct function among entropy generation and exergy destruction as expressed by using the subsequent relation [8]:

$$ex_{DES}^T = T_R S_T^{IRR} \quad (17)$$

A method prolonged to all forms of irreversible processes ought to account for chemical exergy destruction and mechanical exergy destruction, in line with the following generalized model of the Gouy-Stodola theorem:

$$ex_{DES}^G = ex_{DES}^T + ex_{DES}^C + ex_{DES}^M = T_R S_T^{IRR} + \mu_R S_C^{IRR} + p_R V_{RS}^{IRR} \quad (18)$$

That considers the generalized reservoir situations at  $T_R$ ,  $\mu_R$ , and  $p_R$ , ensuring the equality of all thermodynamic potentials and the steady equilibrium state.

The exergy equilibrium calculation of an element is acquired considering the inlet's exergy rate and exiting mass of the equal flow through the control volume. But, in the case of a single circulation coming into without exiting or, vice versa, exiting without an inlet, the exergy assets need to be calculated based totally on the canonical definition to appreciate the outside reference source or surroundings.

The exergy stability is calculated in exergy charge phrases to account for the entire exergy related to mass contributing to the balance of any plant issue. Therefore, for every element, the balance is expressed in phrases of exergy flows.

As far as overall efficiency is involved, the gasoline and product streams are used in the literature to outline the energetic performance is as follows:

$$\eta_{EX}^{OV} = \prod_{j=1}^n \eta_j^{EX} = \prod_{j=1}^n \left( 1 - \frac{EX_D}{EX_{Fj}} \right) = 1 - \frac{EX_D}{\sum_{j=1}^n EX_{Fj}} \quad (19)$$

Where the symbols  $D$  and  $F$  stand for destruction and fuel resource, respectively. Besides, for the sake of clarity and uniformity, the term enter (or inlet) denoted by using the symbol  $IN$  might be utilized here in lieu of fuel resources. Exergy input:

$$EX_{PLS}^{fuel} = EX_{IN}^{BZ,OTSG,Hot} + EX_{IN}^{FW,IHX,hot} + EX_{IN}^{DIV,CAS} + EX_{IN}^{DIV,PFC} + EX_{IN}^{VV} \quad (20)$$

$$EX_{DW}^{fuel} = EX_{IN}^{BZ,OTSG,HOT} + EX_{IN}^{HCSG,HOT} + EX_{IN}^{DIV,CAS} + EX_{IN}^{DIV,PFC} + EX_{IN}^{VV} \quad (21)$$

Exergy Destruction:

$$EX_{PLS}^{fuel} = \Delta EX_{PLS} \text{ and } EX_{DW}^{Des} = \Delta EX_{DW} \quad (22)$$

Exergy fuel source flows taken into consideration are thermal power withdrawn from the Breeding region, First Wall, Divertor Cassette, Divertor plant, and Vacuum Vessel to calculate the exergy rates performance. The pulse-dwell sequence may be taken into consideration as a series of exergy contributions. The exergy efficiency relating to each mode may be calculated in terms of exergy rates. The general exergy performance expression relating to the complete pulse-stay sequence must be obtained in phrases of quantity of exergy calculated alongside pulse and live time intervals. The general exergy performance accounts for the sum of exergy enter and the sum of exergy destruction contributions all through pulse and resides modes. The expression of general exergy efficiency characterizing energy storage system and auxiliary boiler configurations grow to be the following:

$$\eta_{PLS+DW}^{EX} = 1 - \frac{EX_{PLS}^{Des} \cdot \tau_{PLS} + EX_{DW}^{Des} \cdot \tau_{DW}}{EX_{PLS}^{In} \cdot \tau_{PLS} + EX_{DW}^{In} \cdot \tau_{DW}} \quad (23)$$

in which  $\tau_{PLS}$  and  $\tau_{DW}$  are the period of pulse and dwell modes.

## RESULTS AND DISCUSSION

Major phases, pulse, and dwell signify the periodic dynamic thermal power loading and unloading of the molten salt storage device. This exchange operation ensures the regular electric energy input in the grid as an output of the power conversion device (components). Analyses alongside both pulse and dwell strategies account for all additives. The outcomes are produced *via* GateCycleTM, and the spreadsheet is followed to gather all facts and statistics and perform the exergy analyses based totally on the ones previous predesign and balances [11]. The following figures are especially specializing in Breeding blanket Primary Heat Transfer systems. The First Wall Primary Heat Transfer System is directly conveyed to the Once-Through Steam Generator and the power plant to highlight the Primary Heat Transfer System's main components representing the energy carriers' exergy input within the expression of exergy performance. Alternatively, Divertor Cassette, Divertor power components, and Vacuum Vessel additives, used for feedwater preheating in pulse and dwell modes, are duly accounted for in balance efficiencies calculations, especially for each pulse and dwell mode the exergy destruction contributions due to

irreversible phenomena in all plant elements. The thermal exergy variant calculation calls for enthalpy and entropy corresponding to the inlet and outlet states of water, steam, and molten salts. The following figures are acquired from water and steam tables. As concerns, the chemical, physical and thermodynamic characteristics of HITEC reference is made to facts from industrial statistics sheets and literature.

### Dynamic exergy analysis of energy storage system configuration

#### Pulse mode

during the pulse mode (2 hours), the primary cooling water flowing through the plasma chamber's Breeding blanket bar conveys thermal energy, the same as 1481 MWth, to two once through Steam Generator superheated steam is delivered to elements of steam turbines. The Once-Through Steam Generator's main side (high temperature) pressure is 15.4 MPa, and the entire water mass flow charge is 7692 kg/s. The Once-Through Steam Generator secondary aspect (low temperature) pressure is assumed to be 6.40 MPa, and superheated steam is produced and conveyed to the electricity conversion machine (elements). The secondary aspect water mass flow charge consistent with each Once-Through Steam Generator is 812 kg/s. Inlet and outlet temperatures inside the Breeding blanket Once-Through Steam Generator primary (tube-facet, TB) are  $T_{IN}^{BB,OTSG,TB} = 327\text{ }^{\circ}\text{C} = 600\text{ K}$  and  $T_{OUT}^{BB,OTSG,TB} = 294\text{ }^{\circ}\text{C} = 565\text{ K}$  Feedwater coolant inlet and superheated steam outlet temperatures within the Breeding blanket Once-Through Steam Generator Secondary (shell-facet, SH) are  $T_{IN}^{BZ,OTSG,SH} = 237\text{ }^{\circ}\text{C} = 510\text{ K}$  and  $T_{OUT}^{BZ,OTSG,SH} = 298\text{ }^{\circ}\text{C} = 571\text{ K}$ .

The thermal exergy balance of the Once-Through Steam Generator is the consequence of the contributions due to the thermal exergy release along the shell aspect and the thermal exergy growth along the tube side. Consequently, the thermal exergy destruction is calculated by using the subsequent issue balance expression:

$$\Delta EX_{Des}^{BB,OTSG} = \Delta EX_{BB,OTSG,TB}^T + \Delta EX_{BB,OTSG,SH}^T \quad (24)$$

The First Wall Primary Heat Transfer System is designed to get better the thermal electricity 440 MWth produced during the pulse mode (2 h) and use it to save thermal power (1.26 · 107 MJ) within the molten salt with a purpose to be used at some stage in the dwell phase

to supply electric power ensuring the continuity of the electricity output into the electric grid. the 2 Intermediate heat Exchangers switch the thermal strength recovered from the First Wall Primary Heat Transfer System by way of the cooling water flowing inside the main aspect at 15.4 MPa with a mass flow rate of 2271 kg/s, to the HITEC molten salt circulating inside the secondary aspect with a mass flow rate of 4376 kg/s from the low-temperature tank to high-temperature tank.

The 2 Intermediate thermal energy Exchangers are designed to bring thermal energy interplay from First Wall to the molten salt to be saved in the warm tank. The intermediate Heat exchanger's number one aspect (hot) water temperatures are after  $T_{IN}^{FW,IHX,TB} = 327\text{ }^{\circ}\text{C} = 600\text{ K}$  and  $T_{OUT}^{FW,IHX,TB} = 294\text{ }^{\circ}\text{C} = 567\text{ K}$ .

during the two-hour pulse mode, the Intermediate Heat exchanger secondary facet (low temperature) HITEC molten salt mass goes with the flow charge from low temperature to the high-temperature tank is 4376 kg/s . The inlet and outlet temperatures are  $T_{IN}^{FW,IHX,SH} = 281\text{ }^{\circ}\text{C} = 554\text{ K}$  and  $T_{OUT}^{FW,IHX,SH} = 321\text{ }^{\circ}\text{C} = 594\text{ K}$ .

The thermal entropy is calculated thinking that molten salts go through an isovolumic process. Consequently, the expression is  $\Delta S^T = \int_0^1 \frac{C_p}{T} dT \cong \int_0^1 \frac{C_p}{T} dT = C_p \ln \left( \frac{T_1}{T_2} \right) = C_p \ln \left( \frac{T_{OUT}}{T_{in}} \right)$  carried out to practical thermal energy and latent heat throughout melting so that the thermal exergy is  $\Delta \dot{E}X^{FW,IHX,SH} = \dot{m}(\Delta h - T_R \Delta S^T)^{FW,IHX,SH}$  wherein the experimental expression of enthalpy and thermal entropy depending on temperature for molten salt applications is shown in Fig. 1 and reported in the literature [6].

The thermal exergy stability of the Intermediate Heat exchangers consequence of the contributions because of the thermal exergy launch along the shell facet and the thermal exergy increase along the tube aspect. Therefore, the thermal exergy destruction is calculated by way of the following aspect balance expression:

$$\Delta EX_{Des}^{FW,IHX} = \Delta EX_T^{FW,IHX,TB} + \Delta EX_T^{FW,IHX,SH} \quad (25)$$

During the pulse mode, the circulation through the Once-Through Steam Generator and Intermediate Heat exchanger calls for mechanical power to be spent and dissipated along the circuit. The amount of mechanical energy shifting the Breeding blanket cooling water thru the Once-Through Steam Generator shell aspect is 7 MW. As regards the tube side of the Once-Through Steam Generator,

**Table 1: Results of the exergy analysis for the Demonstration fusion power reactor ITER energy storage system in pulse mode.**

Demonstration of fusion power reactor Configuration with energy storage system - Pulse Mode					
PHTS COMPONENT	m (kg/s)	S(kJ/kg.k)	ex(kJ/kg)	$EX_{IN}$ (MW)	$EX_{DES}$ (MW)
BB OTSG Hot Inlet	7617.7233	3.47292	458.0928	3524.895	-44.6886
FW IHX Hot Inlet	2249.28	3.66894	398.8611	906.2064	-4.1679
Divertor Cass. Hot Inlet	852.192	2.39778	179.1702	154.2321	-2.4354
Divertor PFCs Hot Inlet	5264.6715	1.67706	73.1709	389.1096	-6.53895
Vacuum Vessel Hot Inlet	1908.4032	2.30472	162.0234	312.3252	-6.28551

the mechanical electricity results from the contribution of the condenser extraction pump same as 0.4 MW, and the moving pump equal to 5 MW resulting in a complete amount of 5 MW, consequently  $\Delta EX_M^{BZ,OTSG} = 13 MW$ . The power shifting the First Wall cooling water through the Intermediate Heat exchangers tube facet is 2 MW. For the Intermediate Heat exchangers shell aspect, molten salts are moved from the cold tank to the recent tank employing pumps turning in mechanical energy identical to 4 MW, consequently  $\Delta EX_M^{IHX} = 6 MW$ .

in the end, the entire quantity of mechanical strength during pulse mode outcomes in the destruction of mechanical exergy dissipated alongside the motion and ensuing in the pressure loss; the stability of mechanical exergy destruction is subsequent  $\Delta EX_M^{PLS} = \Delta EX_M^{BZ,OTSG} + \Delta EX_M^{FW,IHX} = 18 MW$  the entire exergy balance related to pulse mode consists of the Once-Through Steam Generator and Intermediate Heat exchangers thermal exergy and mechanical exergy charge.

$$\Delta EX^{PLS} = \Delta EX_T^{PLS} + \Delta EX_M^{PLS} \quad (26)$$

Table 1 summarizes the exergy evaluation of this configuration in pulse mode.

#### Dwell mode exergy stability

In addition to the pulse mode case, the thermal exergy balance in stay mode calls for enthalpy and entropy houses similar to the inlet and outlet states of molten salts, water, and superheated steam flowing thru 4 Helical Coil Steam turbines.

The Helical Coil Steam producers are designed to switch the thermal power saved within the high-temperature molten salt to the feedwater to generate the superheated steam to be elevated in steam turbines. All through dwell time of 10 mins, the high-temperature molten salt saved within the high-temperature tank is

added to 4 Helical Coil Steam Generators before being recovered inside the low-temperature tank. The molten salt flows from the high-temperature tank to the low-temperature tank via HCGS shell aspect and releases the thermal energy to the feedwater flowing inside the tube aspect with a mass flow charge of 1021 kg/s (3675 t/h) at 6.4MPa and exits as superheated steam conveyed to be multiplied in steam generators of power components.

The Helical Coil Steam Generator shell facet molten salt temperatures are [3]  $T_{IN}^{HCSG,SH} = 321^\circ C = 594 K$  and  $T_{OUT}^{HCSG,SH} = 554 K$ . The enthalpy is calculated as  $\Delta H^{HCSG,SH} = C_p(T_{OUT}^{HCSG,SH} - T_{IN}^{HCSG,SH})$ ; absolutely, the charge of enthalpy difference is identical during the pulse and dwell phases as no energy accumulation is foreseen in the molten salts. In this situation, the thermal entropy is calculated via the same expression already adopted for the pulse mode in this example expressing an entropy decrease because of cooling, similar to the entropy increase of molten salt heating in the course of the pulse mode. The thermal exergy flow enter needed to calculate the exergy performance is the subsequent:  $EX_{IN}^{PHCSG,TB} = \dot{m}[(h_{IN}^{HCSG,TB} - h_R) - T_R(s_{IN}^{HCSG,TB} - s_R)] = \dot{m} \cdot$

$[c_p(T_{IN}^{HCSG,SH} - T_R) - T_R C_p \ln(\frac{T_{IN}^{HCSG,SH}}{T_R})]$  Feedwater temperature on the tube facet is extended by employing the heat interaction with the molten salt releasing thermal energy. subsequently, from liquid water at  $T_{IN}^{HCSG,TB} = 239^\circ C = 512 K$  to superheated steam  $T_{OUT}^{HCSG,TB} = 300^\circ C = 573 K$  conveyed to the high-pressure steam turbine. Up to now, a thermal exergy balance has been calculated. But, mechanical exergy stability due to pressure loss along interconnecting piping designed to deliver molten salt should be accounted for in pulses and dwell stages to achieve a normal evaluation of thermal and

**Table 2: Exergy analysis results for the Demonstration fusion power reactor ITER using energy storage system in Dwell mode.**

Demonstration fusion power reactor Configuration with ESS - Dwell Mode					
PHTS COMPONENT	m (kg/s)	S(kJ/kg.k)	ex(kJ/kg)	$EX_{IN}$ (MW)	$EX_{DES}$ (MW)
BB OTSG Hot Inlet	10094.4261	3.47292	453.6774	4625.8443	-59.7267
FW IHX+ Hot Inlet	50.4603	3.47292	458.0928	23.3541	-0.31185
Divertor Cass. Hot Inlet	852.192	2.2572	154.2024	132.7392	0.012276
Divertor PFCs Hot Inlet	5264.622	1.64637	69.7653	371.0124	-0.37224
Vacuum Vessel Hot Inlet	1908.4032	2.25819	153.8955	296.6535	-0.32175

mechanical dissipation phenomena inside the energy storage system all through each operating phase. To achieve this, the mechanical exergy destruction charge is calculated to correspond to the mechanical energy delivered by pumps to all circulating fluids. At some point of residing mode, molten salt is moved from the recent tank to the low-temperature tank by pumps delivering mechanical energy equal to 13.9 MW. consequently  $\Delta EX_M^{DW} = \Delta EX_M^{HCSG} = 13.9 MW$  the full exergy balance for the dwell mode duration includes the Helical Coil Steam Generator thermal exergy and mechanical exergy charge.

$$\Delta EX_{DW} = \Delta EX_{DW}^T + \Delta EX_{DW}^M \quad (27)$$

The exergy evaluation in dwell mode is illustrated in Table 2. The thermal power produced within the Divertor Cassette, Divertor power components, and complete Vacuum is conveyed to the regeneration gadget layout to preheat the feedwater earlier than the inlet in the Once-Through Steam Generator during each pulse stay mode and to Intermediate Heat exchangers all through pulse mode only. Preheaters are U-Tubes and Shell thermal energy exchangers.

#### Exergy Efficiency

The Intermediate heat transfer system's general exergy stability, consisting of the energy storage system, is calculated over the two pulses and dwell phases to take a pulse-dwell closed cycle as the reference unit operation. The exergy efficiency is calculated based totally on the exergy quantity throughout every reactor running mode period to evaluate the two phases correctly. Therefore:

$$\Delta EX_{OV} = \Delta EX_{PLS} + \Delta EX_{DW} \quad (28)$$

Pulse Mode: the following expression calculates the exergy performance at some point in pulse mode:

$$\eta^{PLS} = 1 - \quad (29)$$

$$\frac{\sum EX_{Des}}{\sum_{OV}^{p.cs} (E_{in}^{BZ,OTSG,HOT} + E_{in}^{FW,IHX,HOT} + E_{in}^{DIV,PFC} + E_{in}^{VV})}$$

live mode: the exergy performance at some point of dwell mode is calculated with the aid of the following expression:

$$\eta^{PLS} = 1 - \quad (30)$$

$$\frac{\sum EX_{Des}}{\sum_{OV}^{p.cs} (E_{in}^{BZ,OTSG,HOT} + E_{in}^{HCSG,HOT} + E_{in}^{DIV,PFC} + E_{in}^{VV})}$$

#### Dynamic exergy analysis of auxiliary boiler configuration

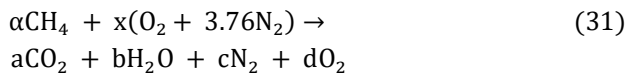
A viable alternative way to reduce plant layout complexity and molten salt tanks and connection piping are to replace the energy storage system with an auxiliary boiler. This fired steam generator is fuelled by natural gas (100% methane  $CH_4$ ) and gives thermal power generation in the dwell section. The thermal design responsibility of this steam generator is about 255 MW as it's far foreseen that, throughout dwell segment, 10% of the mass goes with the flow charge, and as a result, thermal energy is released concerning the pulse segment is considered for plant operation. Furthermore, to keep away from thermal fluctuations and consequent thermal fatigue, the auxiliary steam generator is operated in continuous mode through each pulse and dwell stage to make certain a consistent obligation. This implies that the thermal power released via the auxiliary boiler must be considered all through pulse mode so that thermal power is not used for molten salt heating. Therefore, the whole thermal power produced by the reactor through pulse mode is to be had for the computers and supplied by 4 Once-Through Steam Generators operating in parallel to applying the thermal electricity generated in each breeding zone and first wall. The combustions reaction may be written as follows:

**Table 3: Exergy analysis results for the Demonstration fusion power reactor ITER using Auxiliary boiler in pulse mode.**

Demonstration fusion power reactor Configuration with Auxiliary boiler - Pulse Mode					
PHTS COMPONENT	m (kg/s)	S(kJ/kg.k)	ex(kJ/kg)	EX <sub>IN</sub> (MW)	EX <sub>DES</sub> (MW)
BB + FW	9881.982	3.4749	458.0928	4572.6516	-67.61
OTSG Hot	5.84595	11.4741	49645.53	310.7412	-231.66
Inlet	852.192	2.3958	179.1702	154.2222	-3.3264
Auxiliary	5264.6715	1.6731	73.1709	389.1096	-5.06286
Burner	1908.4032	2.3067	162.0234	312.3252	-6.24888

**Table 4: Exergy analysis results for the demonstration fusion power reactor ITER using an auxiliary boiler in dwell mode.**

Demonstration fusion power reactor Configuration with Auxiliary boiler - Pulse Mode					
PHTS COMPONENT	m (kg/s)	S(kJ/kg.k)	ex(kJ/kg)	EX <sub>IN</sub> (MW)	EX <sub>DES</sub> (MW)
BB + FW	64.6965	3.47292	458.09577	29.93661	-0.50886
OTSG Hot	5.8509	11.4741	49645.53	310.74318	-231.66
Inlet	852.192	2.2572	154.20042	132.73524	-0.010296
Auxiliary	5264.6715	1.64637	69.76827	371.01537	-0.170874
Burner	1908.4032	2.25819	153.89253	296.65548	-0.042471



the standard specific molar chemical exergy of methane, with appreciation to the reference reservoir  $R$  represented by using the surroundings at  $T_R = 298 \text{ K}$  and  $p_R = 101 \text{ kPa}$  is [12]  $ex_{\text{CH}_4}^C = \mu_{\text{CH}_4}(T_R, p_R) - \mu_{\text{CH}_4}^R(T_R, p_R) = 831 \text{ kJ/mol}$  considering the molar weight of methane equal to  $16 \text{ g/mol}$ , then the specific chemical exergy is  $ex_{\text{CH}_4}^C = 52 \text{ J/kg}$ . The methane's lower heating value (LHV) is  $802 \text{ kJ/mol} = 50147 \text{ kJ/kg}$ , the mass flow rate expressed in  $\text{mol/s}$  of methane needed to produce  $255 \text{ MW}$  of thermal power is obtained considering an auxiliary boiler and not using an economizer as preheating is not any needed. Its design implies a lower thermal performance identical to  $\eta_{\text{BOILER}} = 0.861$ . accordingly, the methane mass flow rate is  $\frac{\dot{Q}}{\eta_{\text{BOILER-LHV}}} \cong 368 \frac{\text{mol}}{\text{s}} = 5.9 \frac{\text{kg}}{\text{s}}$  That is the mass flow rate. This is to be accounted for exergy balance with the choice of auxiliary boiler to produce  $255 \text{ MW}$  of thermal electricity. The air mass flow rate, considering air excess of 10%, is equal to  $117 \text{ kg/s}$ . The temperature in the middle of the burning flame inside the combustion

chamber can be assumed at  $2000^\circ\text{C} = 2273 \text{ K}$ . The charge of exergy destruction is calculated as follows:

$$\Delta EX_{\text{DES}} = \Delta EX_{\text{DES}}^T + \Delta EX_{\text{DES}}^C = EX_{\text{IN}} - \Delta EX_{\text{OUT}} \quad (32)$$

in which  $EX_{\text{IN}}$  = heat losses to environment + thermal exergy input + chemical exergy input

$$EX_{\text{IN}} = 282 + 5.9 \cdot 1.05 \cdot 50147 \approx 310942 \text{ kJ/s}$$

$$\Delta EX_{\text{OUT}} = (5.9 + 117) \cdot 957 = 117615 \text{ kJ/s}$$

$$\Delta EX_{\text{DES}} = 310942 - 117615 = 193327 \text{ kJ/s} \approx 194 \text{ MW}$$

Tables 3 and 4 contain all calculated values touching on the auxiliary boiler configuration's pulse and dwell mode.

Further to the energy storage system configuration, the exergy performance is calculated based on the exergy quantity in each reactor working mode inside the case with the auxiliary boiler.

Pulse Mode

$$\eta_{\text{PLS,EX}} = 1 - \frac{\Delta EX_{\text{PLS}}}{\Delta EX_{\text{PLS,fuel}}} = 1 - \frac{\Delta EX_{\text{PLS}}}{\Delta EX_{\text{In}}^{\text{PLS,SH}}} \quad (33)$$

Dwell Mode

$$\eta_{\text{DW,EX}} = 1 - \frac{\Delta EX_{\text{DW}}}{\Delta EX_{\text{DW,fuel}}} = 1 - \frac{\Delta EX_{\text{DW}}}{\Delta EX_{\text{In}}^{\text{OTSG,SH}}} \quad (34)$$

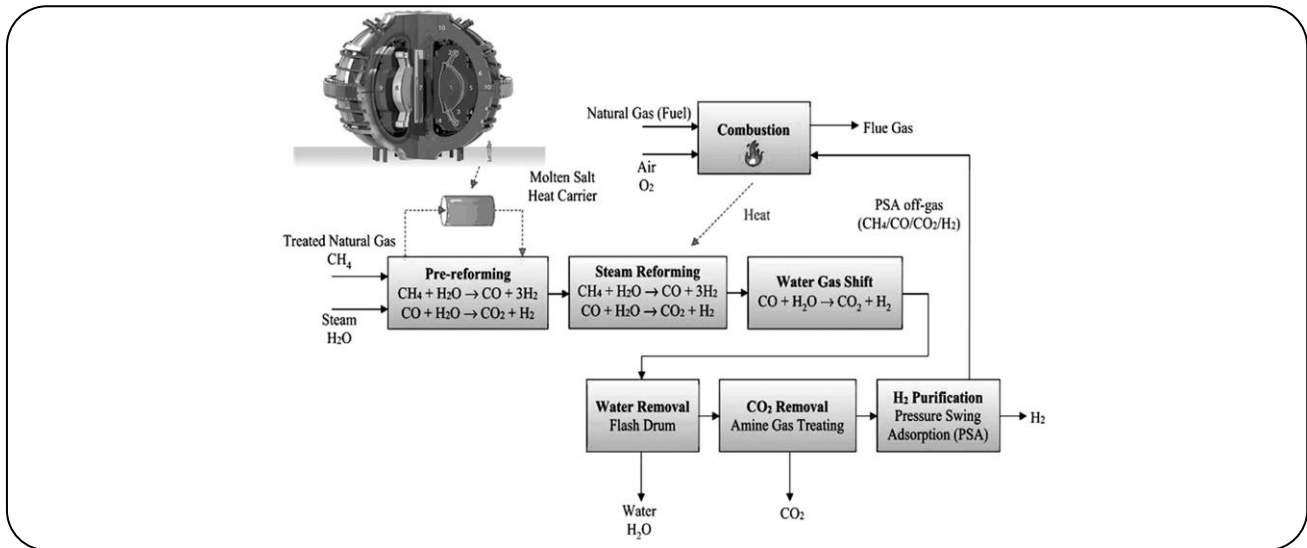


Fig. 3: Schematics of fusion-supported hydrogen generation plant.

### Additional hydrogen production plant

The process used in this paper is almost identical to the conventional process; the additional unit is the pre-reformer unit that utilizes molten salt, heated by a fusion reactor during its pulse modes, as a heat carrier. This pre-reformer partially converts natural gas into hydrogen. Therefore, this will reduce the heat duty required in the main reformer. The rest of the process is no different, as depicted in Fig. 3. The complete results of this equipment, which are implemented in Aspen Plus, are summarized in Table 5.

In Fig. 4a, because the reaction is endothermic, there will be a rapid drop in temperature at the beginning of the reaction due to the need for reactions to high heat flux. Then, as the reactor's heat reaches an equilibrium state, the heat required to react to the reactor temperature decreases with a low slope. Fig. 4b shows the effect of temperature changes on the percentage of methane conversion. As the inlet feed temperature increases, the heat required for the reaction, which is somehow obtained by preheating, is better supplied, increasing the percentage of methane conversion. Fig. 4c shows the three types of reduction, constant and incremental heating methods. Because high-purity raw materials are introduced at the beginning of the reactor, on the other hand, due to the lack of hydrogen in the sweeping gas, the transfer operation in the membrane is better. Thus, the need for heat to react at the beginning of the reactor is less than at the end; as shown in the figure, the conversion rate is the highest when the reaction's heat is low at the beginning of the reaction and then decreases [21-27].

Membrane Permeation Capacity (Cep) is the parameter of membrane penetration capacity in Km, defined as the area of the membrane surface divided by the thickness of the membrane, and the higher the value, the higher the percentage of methane conversion.

The effect of the Cep parameter on the percentage of methane conversion at reactor pressure, steam-to-carbon ratio, and operating temperature is plotted in three separate graphs with Aspen Plus software; this section summarizes the data of these three-figure and shows the results of increasing Cep is the percentage of methane conversion. The complete results of this equipment, which are implemented in Aspen Plus, are summarized in Table 5.

Comparing its cost per unit with other technologies can be the best option to discuss the hydrogen plant results. Electrolysis and steam reforming is the most common technologies to produce hydrogen from water and hydrocarbon, respectively. According to [27], hydrogen generation using electrolysis supported by a geothermal plant is 1.09\$/kg [28]. A firm price cannot be detected in the solar and wind energy plants since each region's electricity generation price is significantly diverse. The thermochemical Cu-Cl reaction by the supercritical steam reactor of fission was studied in [29]. Also, the cost of using seawater is estimated at 2-3.5\$/kg depending on the nuclear system capacity. Also, the thermochemical I-S reaction is investigated by [30], and the cost is estimated at 25.4JPY/Nm<sup>3</sup>. Other nuclear hydrogen systems are also analyzed in another study [31, 32] using high-temperature reactors in which 2.91\$/kg is estimated

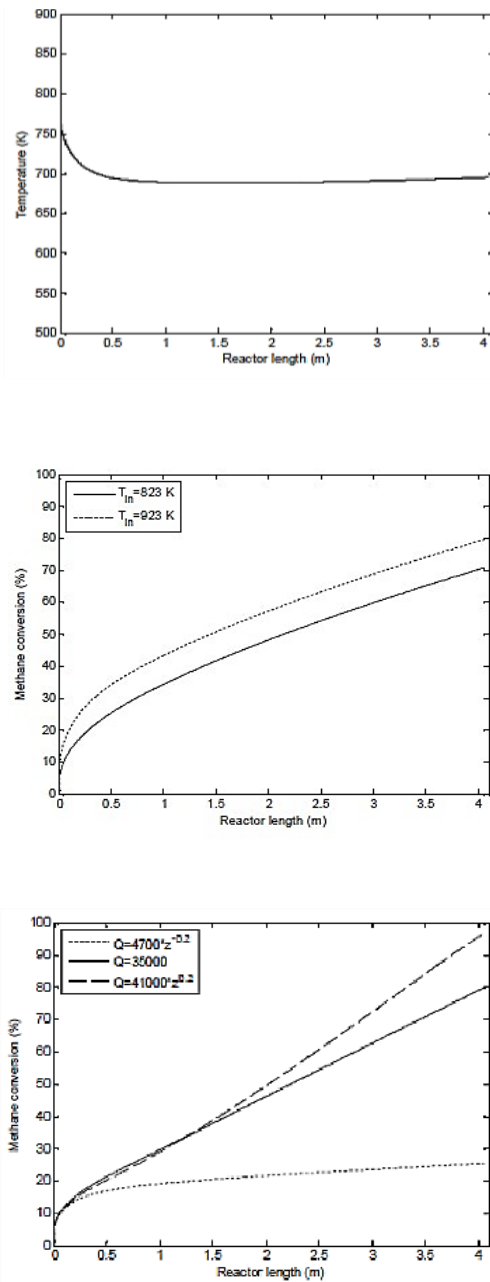


**Fig. 4:** (a) Shows temperature difference in the steam reforming reactor (b) Effect of input temperature on methane conversion percentage (c) Effect of heat transferred to the reactor on methane conversion.

for advanced VVER plant using electrolysis, 2.51\$/kg for high-temperature gas-cooled reactor using electrolysis, and 2.26\$/kg using thermochemical I-S process [33]. The hydrogen cost, including storage and transportation costs, is estimated to reach 3.18-6.17\$/kg.

Also, the photochemical process is used in the biomass conversion method to produce hydrogen. This system was combined with a solar system in a study [34, 35], and the cost was estimated at 2.9\$/kg. Also, the photoelectric chemical cells method is estimated to generate hydrogen at the cost of 15-25\$/GJ [37]. Indirect biophotolysis costs 10\$/GJ, while tubular photo-bioreactor costs 15\$/GJ. The commercial scale of the mentioned technology (photolysis) in algae is shown as a cost of 2.8\$/kg based on 50% capacity [38]. Biomass gasification plants for hydrogen generation cost 8-11\$/GJ (2\$/GJ of biomass cost), but when the scale increases to more than GW, the cost decreases to 6.7-8.4\$/GJ. Cost comparison between reforming processes shows that when we use Small modular reactors to reform methane, the costs are 60% lower than the normal nuclear reactors (3.47\$/kg) [39]. Distributed hydrogen generation is also a more comparative way of hydrogen production, decreasing hydrogen consumer costs by about 50%. However, large-scale high-temperature sources can decrease hydrogen generation costs by more than 80% to ~5\$/GJ (assuming methane price as 13\$/MWh) [40]. Briefly, say, high-temperature, large-scale, and distributed electrolysis or SMR-based hydrocarbon reforming plants are the most probable future of the hydrogen industry because of their significantly lower costs.

### Performance of the plant

The evaluation of performances carried out by the two configurations of the balance of the plant has to summarize the properties alongside both pulse and dwell modes to merge the outcomes in a single indicator, specifically the exergy performance. The efficiency is calculated considering the quantity of exergy input and destruction rather than the costs as previously completed. Then, input and destruction exergy rates need to be accelerated through the pulse and dwell mode length to obtain an exergy quantity summed up and used within the performance expression. For this reason, considering all figures calculated for the energy storage system and auxiliary boiler configuration during the pulse and dwell modes, the subsequent result is received. All results associated with exergy performance above achieved are summarized in the following Table 6:

### Discussion

In this part,  $H_2$  generation potential for ITER systems with SMR, HTE, and S-I processes have been performed.

**Table 5: Simulation results for the hydrogen generation plant using exergy loss of the Demonstration fusion power reactor ITER.**

Parameter	EES	Auxiliary boiler
Conventional Fuel consumption (in reforming)	331.2 ton/h	440.2 ton/h
Water consumption (in reforming)	372.6 ton/h	480.6 ton/h
Electricity consumption	~0	~0
Carbon dioxide production (in reforming)	496.3 ton/h	644.2 ton/h
Heat duty for reactor	254 MW	330MW
Thermal storage required as molten salt	636.5 MW	890.4 MW
Hydrogen production (in reforming)	82.8 ton/h	107.6 ton/h
Carbon emitted to the atmosphere	~0	~0
Levelized cost of hydrogen production	4.8 \$/kg	4.5 \$/kg
Energy efficiency of reforming plant	0.712	0.681
Exergy efficiency of reforming plant	0.706	0.674
Methane conversion factor	0.652	0.667
Energy efficiency of Hydrogen production	0.464	0.455
Exergy efficiency of Hydrogen production	0.652	0.667

**Table 6: Demonstration of fusion power reactor performance.**

Mode	Configuration Parameter	Without hydrogen plant		With hydrogen plant	
		ESS	Auxiliary	ESS	Auxiliary
Pulse	Exergy efficiency	89.70%	85.80%	96.40%	95.30%
	Energy efficiency	88.10%	84.50%	93.62%	91.69%
Dwell	Exergy efficiency	89.40%	73.90%	94.32%	86.01%
	Energy efficiency	88.60%	71.20%	93.89%	84.56%
Overall	Exergy efficiency	89.60%	85.60%	94.43%	92.28%
	Energy efficiency	89.10%	85.07%	94.16%	92.05%
	Levelized Energy Cost	0.096\$/kWh	0.091\$/kWh	0.099\$/kWh	0.093\$/kWh

**Table 7: Hydrogen production rates comparison for different hydrogen generation cycles.**

Reference	Technology	Hydrogen Production Rates (kg/s)				
		SMR			HTE	S-I
		SMR+WGS+MCS	SMR+WGS	SMR		
This research	ITER	72.8	45.2	29.9	6.8	5.7
Ref. [24]	LIFE	17.52	7.94	5.36	0.85	0.69
Ref. [25]	Sombbrero	11.92	5.40	3.64	0.58	0.47
Ref. [26]	FFHR		~33		~11.80	~11.25
Ref. [27]	LIFE				~16.50	
Ref. [28]	LIFE				~1.16	~0.90
Ref. [29]	APEX	~218	~100	~60	~8.60	~8.40
Ref. [30]	3GWR					~94.44

The hydrogen production values for the ITER system obtained for three models of (SMR+WGS+MCS), (SMR+WGS), and (SMR) have been computed as 72.8 kg/s, 45.2 kg/s, and 29.9 kg/s, respectively. When the SMR method is evaluated, the SMR+WGS+MCS system has the highest hydrogen production potential, while the stand-alone SMR has the lowest hydrogen production. The hydrogen production values of the HTE process have been computed as ~7 kg/s for ITER at the end of reactor running time. The hydrogen production values with the S-I process for ITER have been found as ~6 kg/s. When SMR, HTE, and SeI processes are evaluated, the highest hydrogen production with SMR+WGS+MCS system of the SMR process has been obtained as ~220 kg/s for APEX, whereas the lowest hydrogen production has been found with the S-I process as ~0.5 kg/s for Sombbrero. The studies on hydrogen production for different cycles in fusion reactors in recent years are listed in Table 7 a compared [24-30] with the results in the present work. This table also shows validation of the cycle in terms of the productions compared with previous works. As shown in Table 7, hydrogen production varies according to the energy production obtained from the reactor, depending on the fuel, coolants, reactor type, and power. This comparison showed that among the current and previous results obtained by the researchers, it is possible to produce hydrogen from thorium fuel with other alternative fuels using various hydrogen generation cycles and other useful thermal systems [30-34].

## CONCLUSIONS

The present study's primary result is a performance evaluation based on the exergy approach adopted to calculate the balance and efficiency of components and systems constituting the overall plant. The second law of thermodynamics, underpinning the exergy technique, specializes in dissipative phenomena implying entropy production and exergy destruction, representing performance indicators to stumble on the design enhancement. The Primary Heat Transfer System, Intermediate heat transfer system, energy storage system, and plant components of the Demonstration fusion power reactor and balance of the plant assessed using the exergy approach exhibit that the plant's performance was designed with molten salts to stay higher the opportunity solution with an auxiliary boiler replacing the energy storage

system. The difference of exergy efficiency among the solutions here ought to propose the suitability of both configurations. Even though the robust exergo-dissipative combustion response would decrease the performance with the auxiliary boiler on the one facet, the thermal power reduction to 10% throughout dwell mode is mitigated. Although, this answer determines a better strain level and fatigue in steam turbine components. On the opposite side, the energy storage system with molten salt ensures the continuity of complete electricity release; furthermore, this configuration should go through layout enhancements based on optimized shapes of intermediate thermal energy exchangers derived from the entropy generation minimization underpinning the Constructal regulation and Constructal Thermodynamics approach implemented to thermal energy interactions phenomena and heat exchangers layout. Anyway, the most appropriate alternative's choice calls for an extra correct evaluation of plant stability in terms of reliability and economics, considering the plant's place and the need for additional infrastructures. In the final section, a hydrogen plant using exergy loss is designed and analyzed using exergy analysis. The plant results show that this plant's implementation increases the powerplant's efficiency to more than 94% in all modes and configurations, which is a unique achievement of this analysis.

## Nomenclature

c, C	Specific heat, kJ/(kg. K), kJ/(kmol.K)
ex	Specific exergy, kJ/kg, kJ/kmol
EX	Exergy, MJ
$\dot{EX}$	Exergy flow, MW
G, G	Specific Gibbs free energy, kJ/kg, kJ/mol
h,	Specific enthalpy, kJ/kg, kJ/mol
H	Enthalpy, kJ
$\dot{m}$	Mass flow rate, kg/s
n	Number of moles
S	Entropy, kJ/K
T	Temperature, °C, K
u	Specific internal energy, kJ/kg
x	Molar fraction
M	Mechanical
OV	Overall
PLS	Pulse
R	Reference state
REV	Reversible

RR	Restricted Ref.	APEX	Advanced Power EXtraction
SH	Shell side	3GWR	Three Giga Watt Reactor
TB	Tube side	HTE	High-Temperature Electrolysis
T	Thermal		
p, v	Isobaric, isocoric		
OTSG	Once-Through Steam Generator		
PCS	Power Conversion System		
PHTS	Primary Heat Transfer System		
VV	Vacuum Vessel		
SMR	Steam methane reforming		
WGS	water-gas shifts reaction		
MCS	Mineral Carbonation Sequestration		
ITER	International Thermonuclear Experimental Reactor		
HITEC	Commercial name, Eutectic mixture of water-soluble, inorganic salts of potassium nitrate, sodium nitrite, and sodium nitrate		
S-I	Sulfur-Iodine thermochemical water splitting		
p	Pressure, kPa, MPa		
Q̇	Thermal power, MW		
R	Universal gas constant		
s	Specific entropy, kJ/(kg.K)		
v	Specific volume, m <sup>3</sup>		
η	Efficiency, -		
τ	Time interval, s		
μ	Chemical potential, J/mol, kJ/kmol		
C	Chemical		
DES	Destruction		
DW	Dwell		
In	Inlet, input		
IRR	Irreversible		
OUT	outlet		
BOP	Balance of Plant		
BB	Breeding Blanket		
CAS	Cassette		
DEMO	Demonstration fusion power reactor		
DIV	Divertor		
EES	Energy Storage System		
FW	First Wall		
HCPB	Helium Cooled Pebble Bed		
HCSG	Helical Coil Steam Generator		
IHTS	Intermediate Heat Transfer System		
IHX	Intermediate Heat Exchanger		
LHV	Lower Heating Value		
WCLL	Water Cooled Lithium Lead		
LIFE	Laser Inertial Fusion Energy		
FFHR	Force Free Helical Reactor		

Received : Oct. 18, 2022 ; Accepted : Jan. 25, 2023

## REFERENCES

- [1] Federici G., Bachmann C., Biel W., Boccaccini L., Cismondi F., Ciattaglia S., Coleman M., Day C., Diegele E., Franke T., Grattarola M. [Overview of the Design Approach and Prioritization of R&D Activities Towards an EU DEMO](#), *Fusion Engineering and Design*, **109**: 1464-1474 (2016).
- [2] Federici G., Bachmann C., Barucca L., Biel W., Boccaccini L., Brown R., Bustreo C., Ciattaglia S., Cismondi F., Coleman M., Corato V., [DEMO Design Activity in Europe: Progress and Updates](#), *Fusion Engineering and Design*, **136**: 729-741 (2018).
- [3] Bachmann C., Aiello G., Albanese R., Ambrosino R., Arbeiter F., Aubert J., Boccaccini L., Carloni D., Federici G., Fischer U., Kovari M., [Initial DEMO Tokamak Design Configuration Studies.](#), *Fusion Engineering and Design*, **98**: 1423-1426 (2015).
- [4] Linares J.I., Cantizano A., Arenas E., Moratilla B.Y., Martín-Palacios V., Batet L., [Recuperated Versus Single-Recuperator Re-Compressed Supercritical CO2 Brayton Power Cycles for DEMO Fusion Reactor Based on Dual Coolant Lithium Lead Blanket](#), *Energy*, **140**: 307-317 (2017).
- [5] Barucca L., Ciattaglia S., Chantant M., Del Nevo A., Hering W., Martelli E., Moscato I., [Status of EU DEMO Heat Transport and Power Conversion Systems](#), *Fusion Engineering and Design*, **136**: 1557-1566 (2018).
- [6] Malinowski L., Lewandowska M., Giannetti F. [Analysis of the Secondary Circuit of the DEMO Fusion Power Plant Using GateCycle](#), *Fusion Engineering and Design*, **124**: 1237-1240 (2017).
- [7] Zhang K., Du J., Liu X., Zhang H., [Molten Salt Flow and Heat Transfer in Paddle Heat Exchangers](#), *International Journal of Heat and Technology*, **34(1)**: 43-50 (2018).
- [8] Szógrádi M., Norrman S., Bubelis E., [Dynamic Modelling Of The Helium-Cooled DEMO Fusion Power Plant with an Auxiliary Boiler in Apros](#), *Fusion Engineering and Design*, **160**:111970 (2020).

- [9] Bian Z., Wang Z., Jiang B., Hongmanorom P., Zhong W., Kawi S., [A Review on Perovskite Catalysts for Reforming of Methane to Hydrogen Production](#), *Renewable and Sustainable Energy Reviews*, **134**: 110291 (2020).
- [10] Lee B., Kim H., Lee H., Byun M., Won W., Lim H., [Technical and Economic Feasibility under Uncertainty for Methane Dry Reforming of Coke Oven Gas as Simultaneous H<sub>2</sub> Production and CO<sub>2</sub> Utilization](#), *Renewable and Sustainable Energy Reviews*, **133**: 110056 (2020).
- [11] Kulandaivalu T., Mohamed A.R., Ali K.A., Mohammadi M., [Photocatalytic Carbon Dioxide Reforming of Methane as an Alternative Approach for Solar Fuel Production-A Review](#), *Renewable and Sustainable Energy Reviews*, **134**: 110363 (2020).
- [12] Li Z., Lin Q., Li M., Cao J., Liu F., Pan H., Wang Z., Kawi S., [Recent Advances in Process and Catalyst for CO<sub>2</sub> Reforming of Methane](#), *Renewable and Sustainable Energy Reviews*, **134**:110312 (2020).
- [13] Orhan M.F., Dincer I., Naterer G.F., Rosen M.A., [Coupling of Copper–Chloride Hybrid Thermochemical Water Splitting Cycle with a Desalination Plant for Hydrogen Production from Nuclear Energy](#), *International Journal of Hydrogen Energy*, **35**(4): 1560-1574 (2010).
- [14] Iwatsuki J., Kasahara S., Kubo S., Inagaki Y., Kunitomi K., Ogawa M., [Economic Evaluation of HTGR IS Process Hydrogen Production System](#), *Japan Atomic Energy Agency* (2014).
- [15] Yildiz B., Kazimi M.S., [Efficiency of Hydrogen Production Systems Using Alternative Nuclear Energy Technologies](#), *International Journal of Hydrogen Energy*, **31**(1), 77-92 (2006).
- [16] Rodriguez C.A., Modestino M.A., Psaltis D., Moser C., [Design and Cost Considerations for Practical Solar-Hydrogen Generators](#), *Energy & Environmental Science*, **7**(12): 3828-3835 (2014).
- [17] Hisatomi T., Domen K. [Reaction Systems for Solar Hydrogen Production Via Water Splitting with Particulate Semiconductor Photocatalysts](#), *Nature Catalysis*, **2**(5): 387-399 (2019).
- [18] Benemann J.R. [Process “Analysis and Economics of Biophotolysis of Water”](#), *International Energy Agency Hydrogen Implementing Agreement*. (1998).
- [19] Bolton J.R., [Solar Photoproduction of Hydrogen: A Review](#), *Solar Energy*, **57**(1): 37-50 (1996).
- [20] Naterer G., Suppiah S., Lewis M., Gabriel K., Dincer I., Rosen M.A., Fowler M., Rizvi G., Easton E.B., Ikeda B.M., Kaye M.H., [Recent Canadian Advances in Nuclear-Based Hydrogen Production and the Thermochemical Cu–Cl Cycle](#), *International Journal of Hydrogen Energy*, **34**(7): 2901-2917 (2009).
- [21] Karaca A.E., Dincer I., Gu J., [Life Cycle Assessment Study on Nuclear Based Sustainable Hydrogen Production Options](#), *International Journal of Hydrogen Energy*, **45**(41): 22148-22159 (2020).
- [22] Al-Zareer M., Dincer I., Rosen M.A., [Development and Assessment of a Novel Integrated Nuclear Plant for Electricity and Hydrogen Production](#), *Energy Conversion and Management*, **134**: 221-234 (2017).
- [23] Nam H., Nam H., Konishi S., [Techno-Economic Analysis of Hydrogen Production from the Nuclear Fusion-Biomass Hybrid System](#), *International Journal of Energy Research*, **45**(8):11992-2012 (2021).
- [24] Acir A., Asal Ş., [Investigation of the Hydrogen Production of a Laser FUSION Driver Thorium Breeder Using Various Coolants](#), *International Journal of Hydrogen Energy*, **46**(10): 7087-7098 (2021).
- [25] Demir N. [Hydrogen Production Via Steam-Methane Reforming in a SOMBRERO Fusion Breeder with Ceramic Fuel Particles](#), *International Journal of Hydrogen Energy*, **38**(2): 853-860 (2013).
- [26] Özişik G., Demir N., Übeyli M., Yapici H., [Hydrogen Production Via Water Splitting Process in a Molten-Salt Fusion Breeder](#), *International Journal of Hydrogen Energy*, **35**(14): 7357-7368 (2010).
- [27] Adem A.C., Samet A.K., [LIFE Füzyon Reaktöründe Yüksek Sicaklıkta Elektroliz Yöntemi İle Hidrojen Üretimi](#), *Gazi Mühendislik Bilimleri Dergisi (GMBD)*, **5**(1): 1-8 (2019).
- [28] ASAL Ş., ACIR A., [Effect of Hydrogen Generation of The Neutronic Performance in a Laser Inertial Fusion Reactor \(LIFE\) Fuelled Uranium](#), *Journal of Polytechnic-Politeknik Dergisi*, **24**(2): 609-617 (2021).
- [29] Genç G. [Hydrogen Production Potential of APEX Fusion Transmuter Fueled Minor Actinide Fluoride](#), *International Journal of Hydrogen Energy*, **35**(19): 10190-10201 (2010).

- [30] Konishi S., [Potential Fusion Market for Hydrogen Production under Environmental Constraints](#), *Fusion Science and Technology*, **47(4)**: 1205-1209 (2005).
- [31] Hoseinzadeh S., Yargholi R., Kariman H., Heyns P.S., [Exergoeconomic Analysis and Optimization of Reverse Osmosis Desalination Integrated with Geothermal Energy](#), *Environmental Progress & Sustainable Energy*, **39(5)**: e13405 (2020).
- [32] Hoseinzadeh S., Stephan Heyns P. [Advanced Energy, Exergy, and Environmental \(3E\) Analyses and Optimization of a Coal-Fired 400 MW Thermal Power Plant](#), *Journal of Energy Resources Technology*, **143(8)**: 082106 (2021).
- [33] Mahmoudan A., Samadof P., Hosseinzadeh S., Garcia D.A., [A Multigeneration Cascade System Using Ground-source Energy with Cold Recovery: 3E Analyses and Multi-objective Optimization](#), *Energy*, **12**: 121185 (2021).
- [34] Hoseinzadeh S., Ghasemi M.H., Heyns S., [Application of Hybrid Systems In Solution of Low Power Generation at Hot Seasons for Micro Hydro Systems](#), *Renewable Energy*, **160**: 323-332 (2020).
- [35] Norouzi N., Talebi S., [Exergy, Economical and Environmental Analysis of a Natural Gas Direct Chemical Looping Carbon Capture and Formic Acid-Based Hydrogen Storage System](#), *Iranian Journal of Chemistry and Chemical Engineering (IJCCE)*, **41(4)**: 1436-1457 (2022)
- [36] Norouzi N., Hosseinpour M., Talebi S., Fani M., [A 4E Analysis of Renewable Formic Acid Synthesis from the Electrochemical Reduction of Carbon Dioxide and Water: Studying Impacts of the Anolyte Material on the Performance of the Process](#), *Journal of Cleaner Production*, **293**: 126149 (2021).
- [37] Norouzi N., Fani M., Talebi S., [Exergetic Design and Analysis of a Nuclear SMR Reactor Tetrageneration \(Combined Water, Heat, Power, and Chemicals\) with Designed PCM Energy Storage and a CO<sub>2</sub> Gas Turbine Inner Cycle](#), *Nuclear Engineering and Technology*, **53(2)**: 677-687 (2021).
- [38] Norouzi N., Choupanpiesheh S., Talebi S., Khajehpour H., [Exergoenvironmental and Exergoeconomic Modelling and Assessment in the Complex Energy Systems](#), *Iranian Journal of Chemistry and Chemical Engineering (IJCCE)*, **41(3)**: 989-1002 (2022).
- [39] Norouzi N., [An Overview on the Renewable Hydrogen Market](#), *International Journal of Energy Studies*, **6(1)**: 67-94 (2021).
- [40] Norouzi N., [Technical and Economic and Exergy Feasibility of Combined Production of Electricity and Hydrogen Using Photovoltaic Energy](#), *Journal of Applied Dynamic Systems and Control*, **4(1)**: 79-88 (2021).
- [41] Norouzi N., [Thermodynamic and Irreversibility Analysis of the Use of Hydrogen for the Energy Conversion of Fossil Fuel in Power Plants](#), *Journal of Applied Dynamic Systems and Control*, **4(1)**: 97-107 (2021).
- [42] Norouzi N., [Assessment of Technological Path of Hydrogen Energy Industry Development: A Review](#), *Iranian (Iranica) Journal of Energy & Environment*, **12(4)**: 1-2 (2021).
- [43] Norouzi N., Khajehpour H., [Simulation of Methane Gas Production Process from Animal Waste in a Discontinuous Bioreactor](#), *Biointerface Research in Applied Chemistry*, **11(6)**: 13850-13859 (2022).
- [44] Khajehpour H., Norouzi N., Bashash Jafarabadi Z., Valizadeh G., Hemmati M.H., [Energy, Exergy, and Exergoeconomic \(3E\) Analysis of Gas Liquefaction and Gas Associated Liquids Recovery Co-Process Based on the Mixed Fluid Cascade Refrigeration Systems](#), *Iranian Journal of Chemistry and Chemical Engineering (IJCCE)*, **41(4)**: 1391-1410 (2021).
- [45] Norouzi N., Talebi S., Fani M., Khajehpour H. [Exergy and Exergoeconomic Analysis of Hydrogen and Power Cogeneration Using an HTR Plant](#). *Nuclear Engineering and Technology*. **53(8)**: 2753-2760 (2021).